

DESIGN OF RFQ LINAC TO ACCELERATE HIGH CURRENT LITHIUM ION BEAM FROM LASER ION SOURCE FOR COMPACT NEUTRON SOURCE

S. Ikeda*, T. Kanesue, and M. Okamura,
Brookhaven National Laboratory, Upton, NY 11973, USA

Abstract

To develop a high flux neutron source, we propose a linear accelerator systems with lithium beam generated by laser ion source. Because of the higher velocity of center of mass than that in the case of proton beam injection, generated neutrons are directed, and hence the flux is expected to be higher. In this research, we designed RFQ linac optimized to accelerate a high current lithium ion beam.

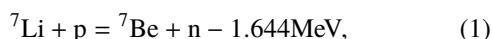
INTRODUCTION

Because the more opportunity of the usage of neutron source are required, compact neutron sources are developed for more conveniently and/or on the spot with lower cost than other neutron sources, such as nuclear reactors and spallation sources and spallation sources. The compact sources can be used to conduct nuclear data measurement [1], non-destructive inspection [2, 3] such as nuclear or explosive material detection in luggage size or cargo size container for security and the defect detection of buildings, and boron neutron capture therapy (BNCT) [4].

As compact neutron sources, there are small neutron generator using D-T reaction, electron linac for photoneuclear reaction, and MeV class proton accelerator with Li or Be target. Among them, the proton accelerator are for high flux neutron generation compared with the others. Linear accelerators are used and developed for the production of MeV class proton beam [5–7]. Typically, the energy range are from 2 MeV to 10 MeV and the current range are from 0.1 mA to 30 mA.

COMPACT NEUTRON SOURCE WITH LASER ION SOURCE

To provide higher neutron flux than conventional sources based on proton accelerators, we propose the linear accelerator using laser ion source. The conceptual design is shown in Fig. 1. The following reaction [8] is used for neutron production,



but lithium ions are injected into a target with protons. The advantage of the lithium injection is the larger center-of-mass velocity compared with proton injection. When proton beam is injected, neutrons are emitted in all direction. Meanwhile, if the lithium beam injected, the neutron scattering angle becomes smaller because the larger center-of-mass velocity

is added to the neutrons, which is expected to lead to higher flux within a solid angle.

The energy threshold of proton for the reaction ${}^7\text{Li}(p,n){}^7\text{Be}$ is 1.881 MeV [8]. Therefore, the energy of lithium needs to be more than 13.1 MeV. In this energy range, IH-Linac is used after RFQ linac typically. For example, the ions are accelerated to 300 keV/u by 3.2-m RFQ, and then 2 MeV/u by 2.5-m linac in injector line for RHIC in Brookhaven National Laboratory [9].

A solid lithium target are placed in the plasma production chamber as shown in Fig. 1. Ablation plasma containing Li^{3+} is produced by irradiation on the target with focused pulsed laser. The advantage of laser ion source is capability of producing 10 mA-class beam of fully stripped ion. In previous work, it was found that Li^{3+} can be produced by a table top laser.

After the production, the plasma drifts in the direction normal to the target surface and then is injected into the RFQ linac directly without low energy beam transport line. Since the plasma production chamber is charged up, the ion beam is extracted at the entrance of the RFQ linac. Typically, low energy transport line between ion source and RFQ linac is the problem for high current heavy ion beam acceleration. The space charge problem is avoided by injecting the drifting plasma into the RFQ linac directly. In a previous work, 20 mA of C^{6+} was accelerated using this scheme [10].

The accelerated beam is focused and bunched in MEBT line before injected into IH-linac in which the ions are accelerated to 13 MeV or more. Then the beam is injected in to the target containing proton, such as hydrogen gas, water, or Titanium hydride to produce neutron beam.

As a first step, we designed the RFQ linac to accelerate for high current beam of ${}^7\text{Li}^{3+}$ to 300 keV/u prioritizing output current rather than transmission. We used the simulation code, PARMTEQ.

RFQ DESIGN VALUES AND CALCULATION RESULTS

Table 1 shows the summary of the RFQ design parameters. The frequency was set as 100 MHz for high current beam acceleration. The input energy was determined from the previous laser ion source experiments in which the extraction voltage was 60 kV. The energy is also close to the typical RFQ injection energy. Mass to charge of ${}^7\text{Li}^{3+}$ is 3/7. Input transverse normalized total emittance was set as 1π mm mrad, and particle distribution was assumed to be four dimensional water bag. Input twiss parameter β was determined as the beam radius was the same as the minimum

* siked@bnl.gov

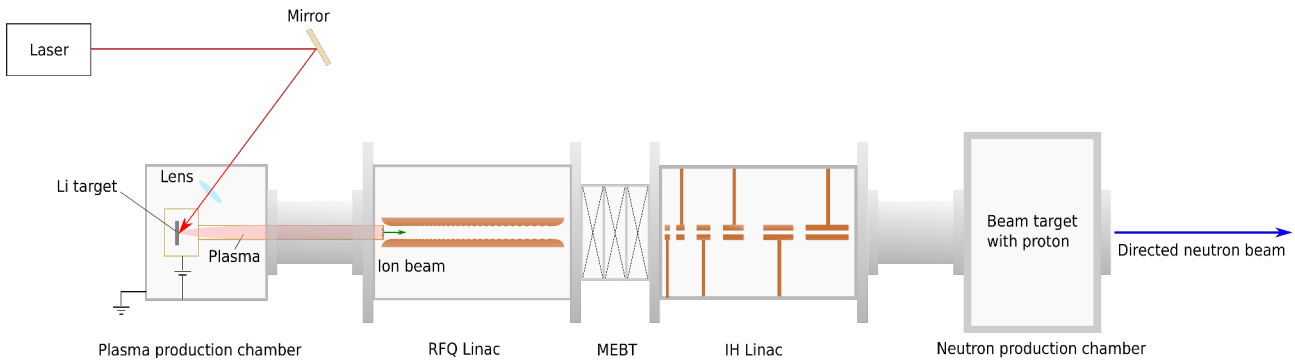


Figure 1: Conceptual design of compact neutron source using laser ion source.

tip radius a using the relation $\sqrt{\beta\epsilon} = a$. It was assumed that the input energy spread was zero and phase spread was ± 180 degree. The vavoltage was set as the value with which the surface electric field is twice as high as that calculated from Kilpatrick criterion. Synchronous phase in acceleration section was set as -30 degree. Under these conditions, we adjusted a , the input twiss parameter α , and the beam current to obtain the high output beam current.

Table 1: RFQ design parameters

Frequency	100 MHz
Input energy	0.026 MeV/u
Output energy	0.3 MeV/u
Mass to charge ration	3/7
Input beam current	50 mA
Input trans. norm. total emittance	1π mm mrad
Input particle distribution	4D water-bag
Input twiss parameter α	3.8
Input twiss parameter β	18.6 cm/rad
Input Energy spread	± 180 deg
Input phase spread	0 degree
Bravery factor	2
Vane voltage	120 kV
Minimum radius	0.5 cm
Final modulation factor	2.4
Synchronous phase	-30 deg
RFQ length	2.3 m
Cell number	151
Transmission	80 %
Output current	40 mA
Output trans. norm. rms emittance	0.044π cm mrad

Figure 2 shows the adjusted cell parameters as a function of the distance from the end of the radial matching section that contains of first four cells with the length of 5.6 cm. The shaper section is from there to 67 cm. In the section, the modulation factor increases from 1 to 1.13 proportionally while the synchronous energy increases from 0.180 to 0.205 MeV and the minimum radius a decreases from 0.84 to 0.79 cm. The bunching section is to 223 cm. The modulation factor increases to 2.4 while the energy increases to 1.96 MeV and a decreases to 0.47 cm. Then acceleration region

follows to 227 cm. The vane voltage is 120 kV. From the values the coefficients A_0 and A_{10} are calculated as shown in Fig. 2. The total cell number and length are 152 and 230 cm, respectively. The relation is shown in Fig. 3. The distance increases almost linearly to the cell number from 0 to around 60 while the distance increases more steeply after 60. This is because the buncher section starts around 60, and hence the cell length become longer as the beam is accelerated. 97 % of the designed RFQ linac is for the bunching and 1.7 % is for the acceleration.

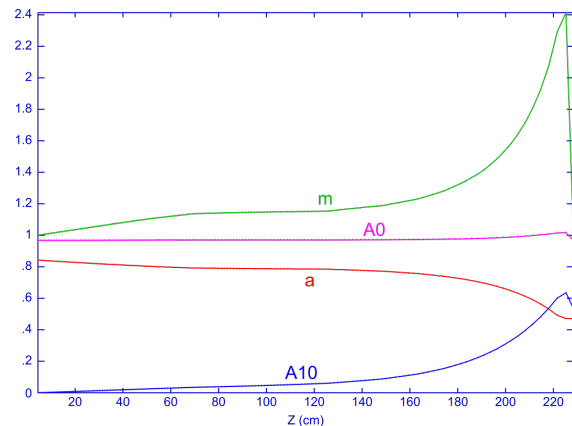


Figure 2: Cell parameters as a function of the distance from the entrance of the RFQ linac.

The results of the calculation of the beam dynamics are shown in Fig. 4. Fig. 4(a) and 4(b) display the particle transverse positions x and y , respectively. Although the envelopes in x and y directions oscillate, which may show the beam is not matched well, most of the particles are inside of the minimum tip radius a . Fig. 4(c) and 4(d) show the differences of the phase ϕ from the synchronous phase ϕ_s and the energy w from the synchronous energy w_s . As shown in Fig. 4(d), the particles that have negative value of $w - w_s$ around number 60 become slower and lost from the figure between the cell number 60 to 110. This is because the bunching section starts around number 60. After that the synchronous phase increases, and then the cell length become larger with the increase of the cell number as shown in the steep increase of the distance in Fig. 3. Therefore,

4: Hadron Accelerators

A08 - Linear Accelerators

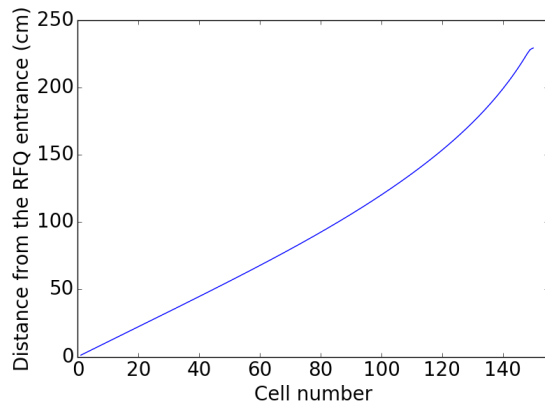


Figure 3: Distance from the RFQ entrance as a function of the cell number.

the decrease of the $w - w_s$ means that some particles can not be accelerated from number 60. This is the main cause of beam loss. Because the beam loss decreases when the beam current is reduced, the failure of acceleration of some particles is due to the space charge effect.

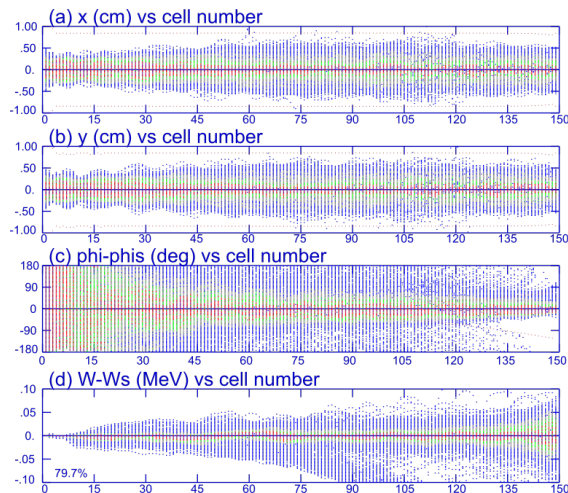


Figure 4: Calculated particle parameters, x (a), y (b), phase difference $\phi - \phi_s$, and energy difference $W - W_s$ as a function of the cell number.

As described in Table 1, the transmission is 80 % and the output current is 40 mA. The output transverse and normalized rms emittance is 0.044π cm mrad. 90 % particles are included with the emittance 5 times as large as the rms value. On the basis on the results, we will investigate the feasibility of producing the lithium beam with the current of 40 mA for the compact neutron source with laser ion source.

CONCLUSION

We proposed a compact neutron source by means of lithium injection using laser ion source. For high current lithium ion acceleration, we surveyed a RFQ desing parameters. We found the design with which 40 mA lithium ion will be accelerated to 300 keV/u in 2.3 m.

ACKNOWLEDGMENT

This work was supported by the US Department of Energy under contract number DE-SC0012704.

REFERENCES

- [1] T. Matsumoto, M. Igashira, and T. Ohsaki, "Measurement of kev-neutron capture cross sections and capture gamma-ray spectra of 99tc," *J. Nucl. Sci. Technol.*, vol. 40, no. 2, pp. 61–68, 2003.
- [2] J. Harmon, D. Wells, and A. Hunt, "Neutrons and photons in nondestructive detection," *Rev. Accelerator Sci. Technol.*, vol. 4, no. 01, pp. 83–101, 2011.
- [3] M. Takamura *et al*, "Non-destructive texture measurement of steel sheets with compact neutron source "rans"," in *J. Phys. Conf. Ser.*, vol. 734, no. 3. IOP Publishing, 2016, p. 032047.
- [4] D. W. Nigg, "Some recent trends and progress in the physics and biophysics of neutron capture therapy," *Prog. Nucl. Energ.*, vol. 35, no. 1, pp. 79–127, 1999.
- [5] A. Kreiner *et al.*, "Accelerator-based bnct," *Appl. Radiat. Isotopes*, vol. 88, pp. 185–189, 2014.
- [6] M. Yoshioka, "Review of accelerator-based boron neutron capture therapy machines," in *7th Int. Particle Accelerator Conf. (IPAC'16)*, Busan, Korea, May, 2016, THXB01, pp. 3171–3175.
- [7] M. Uesaka and H. Kobayashi, "Compact neutron sources for energy and security," *Rev. Accelerator Sci. Technol.*, vol. 8, pp. 181–207, 2015.
- [8] H. Liskien and A. Paulsen, "Neutron production cross sections and energies for the reactions $7\text{Li}(p, n)7\text{Be}$ and $7\text{Li}(p, n)7\text{Be}$," *Atom. Data Nucl. Data*, vol. 15, no. 1, pp. 57–84, 1975.
- [9] A. Schempp *et al.*, "RFQ and IH accelerators for the new EBIS injector at BNL", in *Proc. 22nd Particle Accelerator Conf. (PAC'07)*, Albuquerque, New Mexico, USA, June, 2007, TUPAN021, pp. 1439–1449
- [10] H. Kashiwagi *et al.*, "Acceleration of high current fully stripped carbon ion beam by direct injection scheme," *Rev. Sci. Instrum.*, vol. 77, no. 3, 2006.